Metal Nanoparticle Pollutants Interfere with Pulmonary Surfactant Function In Vitro

Mandeep Singh Bakshi,*†§‖ Lin Zhao,* Ronald Smith,‡ Fred Possmayer,*† and Nils O. Petersen†§¶
*Department of Obstetrics and Gynaecology, †Department of Biochemistry, ‡Department of Biology, and §Department of Chemistry, University of Western Ontario, Schulich School of Medicine and Dentistry, London, Ontario, Canada; ¶National Institute for Nanotechnology, Edmonton, Alberta, Canada; and ‖Department of Chemistry, Guru Nanak Dev University, Amritsar, India

ABSTRACT Reported associations between air pollution and pulmonary and cardiovascular diseases prompted studies on the effects of gold nanoparticles (Au NP) on pulmonary surfactant function. Low levels (3.7 mol % Au/lipid, 0.98% wt/wt) markedly inhibited adsorption of a semisynthetic pulmonary surfactant (dipalmitoyl-phosphatidylcholine (DPPC)/palmitoyl-oleoyl-phosphatidylglycerol/surfactant protein B (SP-B); 70:30:1 wt %). Au NP also impeded the surfactant's ability to reduce surface tension (γ) to low levels during film compression and to respread during film expansion. Transmission electron microscopy showed that Au NP generated by a seed-growth method were spherical with diameters of ~15 nm. Including palmitoyl-oleoyl-phosphatidylglycerol appeared to coat the NP with at least one lipid bilayer but did not affect NP shape or size. Similar overall observations occurred with dimyristoyl phosphatidylglycerol. Dipalmitoyl-phosphatidylglycerol was less effective in NP capping, although similar sized NP were formed. Including SP-B (1% wt/wt) appears to induce the formation of elongated strands of interacting threads with the fluid phosphatidylglycerols (PG). Including DPPC resulted in formation of aggregated, less spherical NP with a larger size distribution. With DPPC, strand formation due to SP-B was not observed. Agarose gel electrophoresis studies demonstrated that the aggregation induced by SP-B blocked migration of PG-coated NP. Migration was also influenced by the fluidity of the PGs. It is concluded that Au NP can interact with and sequester pulmonary surfactant phospholipids and, if inhaled from the atmosphere, could impede pulmonary surfactant function in the lung.

INTRODUCTION

Pulmonary surfactant is essential for normal lung function (1–3). Surfactant forms a surface-active film composed primarily of phospholipids (PL) that coat the air/water hypophase covering the alveolar tissue surface. By lowering surface tension (γ) to near equilibrium during inspiration, surfactant minimizes the work of breathing. By reducing γ to low values during expiration, surfactant stabilizes the lung at low lung volumes and limits the tendency to develop pulmonary edema. Mammalian surfactants contain ~90% lipid and ~10% surfactant-specific proteins SP-A, SP-B, SP-C, and SP-D. Of these, SP-A and SP-D are large, hydrophilic oligomeric proteins that function primarily in host defense, whereas SP-B and SP-C are low molecular weight hydrophobic proteins that markedly alter the surface properties of surfactant PL (4–9).

Phosphatidylcholine (PC) and phosphatidylglycerol (PG) are major surfactant PLs. PLs are hydrophobic amphipathic substances that spontaneously form vesicles but adsorb and spread only slowly at the air-liquid interface. This is particularly true of gel phase PLs, such as the principal surfactant molecular species dipalmitoyl-phosphatidylcholine (DPPC) below its bilayer gel to liquid-crystalline phase transition temperature of 41°C. Both SP-B and SP-C enhance adsorption and spreading of surfactant lipids at the air-liquid interface. SP-B and SP-C also affect the compressibility of surfactant PL films, thereby permitting such films to attain low γ-values near 0 mN/m. Such low surface tensions are required for the normal breathing process (1–3).

Not surprisingly, factors affecting surfactant impact on pulmonary function. Surfactant deficiency, such as can occur with premature delivery, can lead to development of the respiratory distress syndrome (RDS), an important cause of perinatal morbidity and mortality (10,11). Surfactant dysfunction also contributes to significant morbidity and mortality with acute lung injury (ALI) and the acute respiratory distress syndrome (ARDS) (12,13). ALI and ARDS rise from a number of causes and with these diseases, surfactant dysfunction is usually, if not always, a secondary effect.

Although the mechanisms involved are not always clear, considerable evidence has accumulated indicating that pulmonary function and cardiovascular function can be dramatically affected by air pollution (14–19). It is apparent that fine (<250 nm) and ultrafine (<100 nm) airborne particles can be conducted to the terminal air spaces. However, little is known about the effects of air pollutants on pulmonary surfactant function. Therefore, in this study, we examined the effects of chemically generated gold nanoparticles (Au NP), as a model air pollutant, on surfactant function using an artificial alveolar model, the captive bubble tensiometer (CBT). The surfactant used was DPPC/palmitoyl-oleoyl-phosphatidylglycerol (POPG)/SP-B (70:30:1; wt/wt/wt), a semisynthetic system that displays many of the basic

Submitted February 16, 2007, and accepted for publication August 29, 2007.

Address reprint requests to Fred Possmayer, Depts. of Obs/Gyn and Biochemistry, Schulich School of Medicine and Dentistry, DSB 5009, London, ON, Canada N6A 5C1. E-mail: fpossmay@uwo.ca.

Editor: Thomas J. McIntosh.

0006-3495/08/02/855/14 $2.00

doi: 10.1529/biophysj.107.106971

properties of natural pulmonary surfactant (20–27). It was observed that mixing extremely low numbers of Au NP, <1% wt/wt, with the surfactant system greatly impeded surfactant PL adsorption. Furthermore, the NP interfered with the ability of surfactant films to achieve low γ-values during quasistatic or dynamic film compression and to respread to maintain relatively low γ-values during surface area expansion. These observations prompted a further examination of the interactions between the major surfactant PL constituents and Au NP. The effect of SP-B, a critical surfactant apoprotein previously demonstrated to be essential for normal gaseous exchange, on PL/Au NP interactions was also investigated. In both cases, highly specific interactions were noted between the surfactant constituents. In keeping with previous studies, it appeared that Au NP become ''capped'' in the presence of acidic surfactant phospholipids. This interaction was markedly altered in the presence of SP-B, which resulted in highly aggregated Au NP. This latter observation may, in part, explain the highly deleterious effect of the NP on the ability of surfactant PL to adsorb and to reduce surface tension to low values, as determined during surface area expansion/compression cycling.

EXPERIMENTAL

Materials

Standard chemicals were from VWR (Mississauga, Ontario, Canada), unless noted. Tetrachloroauric acid ($HAuCl_4$), sodium borohydride ($NaBH_4$), and trisodium citrate were obtained from Sigma/Aldrich (Oakville, Ontario, Canada). 1,2-dipalmitoyl-*sn*-glycero-3-phosphocholine (DPPC), 1,2-dimyristoyl-phosphatidylcholine (DMPC), 1-palmitoyl-2-oleoyl-*sn*-glycero-3-[phospho-*rac*-(1-glycerol)] (sodium salt) (POPG) (16:0-18:1), 1,2-dipalmitoyl-*sn*-glycero-3-[phospho-*rac*-(1-glycerol)] (sodium salt) (DPPG) (di-16:0), and 1,2-dimyristoyl-*sn*-glycero-3-[phospho-*rac*-(1-glycerol)] (sodium salt) (DMPG) (di-14:0) were procured from Avanti Polar Lipids (Birmingham, AL). The pulmonary SP-B was isolated from a clinical surfactant, bovine lipid extract surfactant (BLES), as described earlier (28). Ultrapure water was used for all aqueous preparations.

Preparation of lipid-capped gold nanoparticles

The Au NP and lipid-capped Au NP were prepared by the seed growth (S-G) method. For the seed solution, 20 ml of 0.5 mM $HAuCl_4$ aqueous solution were taken in a screw-capped glass bottle and dry sodium citrate was added to make a final concentration of 0.5 mM. Then, 0.6 ml of aqueous 0.1 M $NaBH_4$ solution were added under constant stirring, giving rise to a ruby red color in the final solution, which acts as the seed solution. The growth solution was prepared by taking 120 μg of lipid (1 mg/ml) in chloroform or as otherwise specified, in a glass screw-capped tube. The chloroform was evaporated under the flux of pure N_2 leaving a dried lipid film around the bottom of the tube. Pure water (5 ml) was added along with two to three small glass beads and the tube was vortexed for several minutes to completely disperse the lipid in the aqueous phase. This was followed by the addition of $HAuCl_4$ so as to make $[HAuCl_4] = 0.5$ mM, which gave a light yellow color to the solution. Then, 0.5 ml of the previously prepared seed solution was added, followed by 0.2 ml of freshly prepared 0.1 M aqueous ascorbic acid solution. This addition gave an instant deep ruby red color to the suspension. The suspension was mixed by inverting the tube several times and kept in the dark without disturbing it at least for 2 days. Control noncoated blank Au NP particles were prepared as above, but omitting the PL. The pH of the NP suspensions was always close to neutral in each case.

Purification of each aqueous sample of control and lipid-capped NP was carried out by repeated washing at least 3–4 times with ~10 ml distilled water by centrifugation at 10,000 rpm for 10 min, pouring off the supernatant and redispersing the precipitate in H_2O each time to remove soluble chemicals.

Analytical methods

Captive bubble tensiometry

The surfactant suspensions were made by mixing the constituents (DPPC/POPG; 70:30 with and without 1% SP-B) in chloroform and drying the resulting solution with a stream of dry nitrogen to form a thin film on the walls of a glass tube. The dried surfactant films were then dispersed within the following buffer (in mM): 150 NaCl, 2 Tris-HCl, pH 7.4, and 1.5 $CaCl_2$, to give a final lipid concentration of 200 μg/ml. The surface properties of these suspensions were then studied with and without addition of naked (i.e., nonlipid-capped) Au NP. Samples were incubated at 37°C for at least 1 h before being inserted in the CBT chamber as below.

Surface properties were examined employing a custom-designed CBT as described previously (24,29). Briefly, after filling the chamber and allowing it to equilibrate to 37 ± 1°C, an air bubble (~8 mm diameter) was sucked into the suspension at atmospheric pressure. The bubble rose to rest against a hydrophilic agar plug that apparently eliminates any detectable loss of surface-active material (i.e., so-called film leakage). Changes in bubble shape were recorded with a video camera for 1 h or until the PL equilibrium γ (γ_{eq}) of ~23 mN/m was attained. In some cases where γ_{eq} was not attained, the duration of the adsorptive phase was prolonged. After adsorption, the bubble chamber was sealed and the surface area of the bubble was systematically compressed and expanded in either quasistatic or dynamic modes (30 cycles/min), as described previously (24,30). Images documenting alterations in bubble shape were recorded continuously and were subsequently analyzed using custom designed software (31).

Quasistatic experiments were conducted by increasing the pressure in the sample chamber stepwise, such that the relative bubble area decreased, and waiting 10 s between steps. We conducted three quasistatic cycles with an intercycle delay of 1 min to allow reequilibration of the system. With control surfactant, the bubble progressively flattened, indicating lower γ. The minimum γ (γ_{min}) was achieved when the bubble decreased in size with no further reduction in γ. Overcompression was avoided wherever possible. Dynamic cycles were conducted by setting the bubble volume limits on the basis of the quasistatic compression-expansion cycles and then cycling the bubble between these relative bubble surface areas $\pm 20\%$ at 10 cycles/min.

All experiments were performed at least 3 times using individual freshly prepared samples. Standard deviation of the mean was obtained from $n = 3$ or more sets of data, using separate samples. Statistical analysis was done using analysis of variance techniques and Tukey's honestly significant difference test for multiple comparisons among the reconstituted surfactants.

Ultraviolet spectroscopy

Ultraviolet-visible (UV-vis) spectra of the prepared samples were taken by a UV spectrophotometer (Multiskan Spectrum, Thermo Fisher Scientific, Waltham, MA) in the wavelength range of 200–900 nm. The formation of Au NP was monitored in the visible absorption range of ≈530 nm. The shape and size of the gold NP were characterized by transmission electron microscopy (TEM). Samples were prepared by mounting a drop of aqueous NP suspension on a carbon-coated Cu grid and allowing it to dry in air. Samples were then observed with the help of a Philips CM10 transmission electron microscope (Eindhoven, The Netherlands) operating at 100 kV.

Gel electrophoresis

The polarity of the lipid-capped NP samples was determined by gel electrophoresis using TBE (tris-borate, 90 mM; ethylene diamine tetraacetic acid (EDTA), 2 mM, pH 8.0) buffer as a gel running medium. For this purpose, 1% of aqueous agarose solution was first heated to boiling with a microwave, poured into a gel plate, and allowed to harden. Then 20 μl of aqueous NP solution was loaded in each gel well and a direct voltage of 90 V was applied for 10 min to promote the movement of NP. No staining agent was needed because the NP solutions in each case were colored (either pink or purple).

RESULTS

Effect of Au NP on pulmonary surfactant function

Initial studies investigated the potential effects of Au NP as a model metal air pollutant on pulmonary surfactant. A chemically defined semisynthetic surfactant composed of DPPC/POPG/SP-B (70:30:1) was employed because this system is chemically defined and has been extensively characterized by our group and others (20–27). The effect of Au NP as an air pollutant was studied by adding blank, naked (i.e., noncapped) NP to suspensions of DPPC/POPG/SP-B (70:30:1). The surface activity of these surfactant systems was then determined with the help of a CBT. Fig. 1 shows that DPPC/POPG (70:30) suspensions (*open circles*) at 200 μg/ml initially adsorb relatively rapidly, thereby lowering γ from 70 mN/m (H_2O at 37°C) to reach $\gamma \approx 40$ mN/m by 30 min with little further change to 60 min. Inclusion of 1% SP-B (*squares*) clearly augmented adsorption such that the surfactant system reached the equilibrium γ (γ_{eq}) of 23 mN/m at ~15 min. Addition of various amounts of naked Au NP to DPPC/POPG/SP-B mixtures led to a decrease in adsorption. At a PL/Au mol ratio of 27 (i.e., $[DPPC/POPG]/[Au] = 27$), corresponding to 3.7 mol % or with 0.98% wt/wt Au, the lowest concentration examined, surfactant adsorption was drastically impeded so that γ decreased only slowly to ~52 mN/m within 60 min (*diamonds*). The adsorption in the presence of Au NP was considerably slower and less complete than in the absence of SP-B.

To maintain normal pulmonary function, surfactant films must achieve low γ near zero during expiration (i.e., compression) and maintain γ-values near equilibrium during inspiration (i.e., surface area expansion). Figs. 2 and 3 show quasistatic cycles (first and third) and dynamic cycles (first and 21st), which are designed to mimic the expansion-compression cycling of the alveolar surface during breathing. Progressive quasistatic compression (*solid circles*) of adsorbed DPPC/POPG/SP-B (70:30:1) films (Fig. 2 *a*) led to a slow and then more rapid reduction in γ until surface

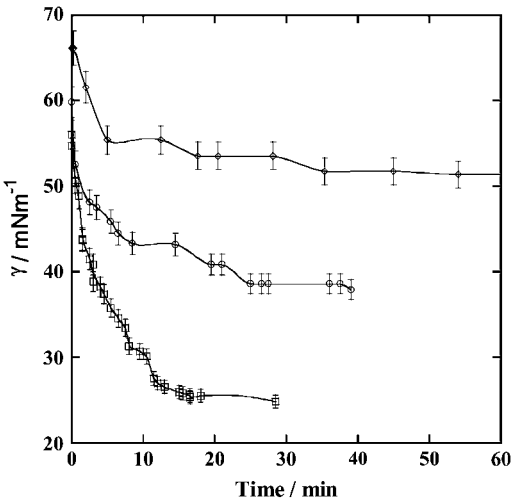

FIGURE 1 Adsorption isotherms of DPPC/POPG (70:30) (*circles*), DPPC/POPG/SP-B (70:30:1) (*diamonds*), and DPPC/POPG/SP-B with control, noncapped Au NP (3.7 mol % Au/PL) (*squares*). Isotherms were obtained by monitoring the adsorption of 200 μg/ml of lipid, lipid-protein, or lipid-protein-NP mixtures in the captive bubble tensiometer at 37°C.

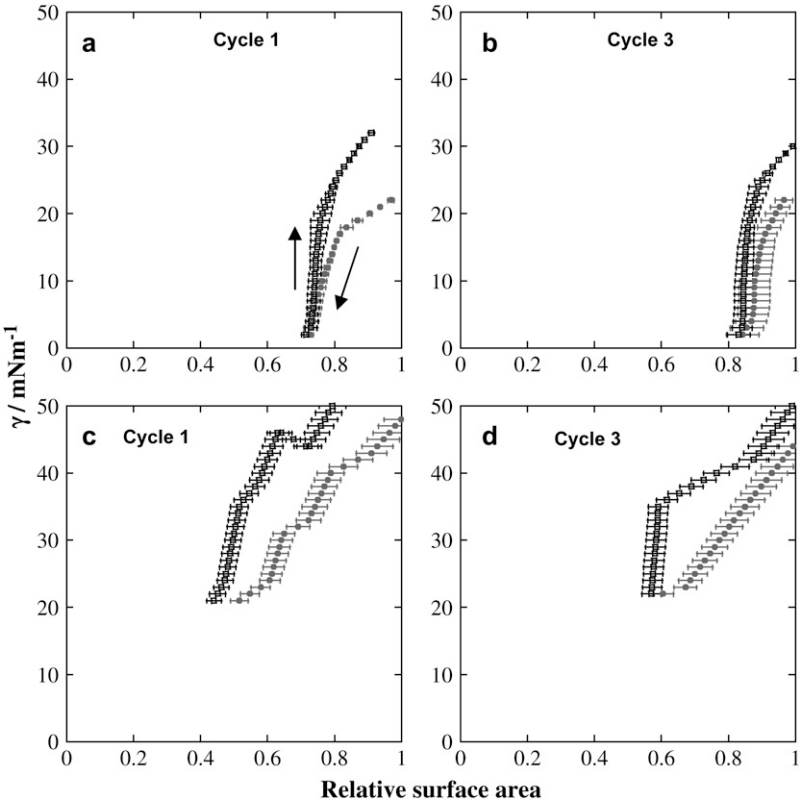

FIGURE 2 Quasistatic compression (●)-expansion (○) isotherms of DPPC/POPG/SP-B (70:30:1) during the first (*a* and *c*) and third (*b* and *d*) cycles, in the absence (*a* and *b*) or presence (*c* and *d*) of blank Au NP (3.7 mol % PL). The arrows in panel *a* indicate surface area expansion (*up*) or reduction (*down*).

tensions of <2 mN/m are attained with a surface area reduction of ~30%. Film expansion (*open squares*) resulted in an immediate and then more gradual increase in γ to values of ~30 mN/m at the original bubble size. By the third quasistatic cycle (Fig. 2 *b*), γ reduction during compression occurs more directly and surface area reductions of ~15% are sufficient to attain γ-values near zero. This is only slightly larger than the 12% surface area reductions observed with DPPC films (1). Furthermore, the γ-values exhibited during film expansion remain lower than observed at the same relative areas in the initial cycle. These observations indicate the film has somehow become refined during surface area cycling.

Adding naked Au NP to the surfactant mixture resulted in a marked deterioration in surface film properties. Fig. 2 *c* demonstrates that compression of surfactant films in the presence of Au NP particles (3.7 mol %, 0.98% wt/wt PL) greatly hampered γ reduction during film compression from ~45 mN/m. Reducing the surface area by half resulted in a γ_{min} of ~23 mN/m, similar to the γ_{eq} obtained with the pure surfactant system. Further compression did not result in a corresponding reduction in γ_{min} (not shown). Such overcompression was avoided in the results depicted here. Film expansion led to γ_{max} values >50 mN/m. By the third cycle, compressibility was slightly improved but γ_{min} remained at ~23 mN/m. Surface tension reduction during film expansion was also slightly improved, as indicated by an expansion plateau near 40 mN/m, but γ_{max} still remained at ~50 mN/m. In other studies, with prolonged adsorption where film compression was initiated at ~40 mN/m, γ_{min} still remained at ~20 mN/m with cycles 1 and 3.

Similar overall results were obtained with control surfactant during dynamic experiments at 30 cycles/min, which more closely mimic the normal breathing process (Fig. 3). Low γ_{min} values of <2.0 mN/m were achieved during compression with both dynamic cycles 1 and 21. In each case, <20% surface area reduction was required. The γ_{max} values were ~30 mN/m, showing that surfactant PL response was similar to that observed with quasistatic cycle 3. Hysteresis was minimal, especially with cycle 21. Inclusion of Au NP (3.7 mol %) resulted in γ_{min} values of ~20 mN/m, similar to those observed with the quasistatic studies. Although some improvement was observed with compression/expansion cycling, the γ_{max} values were high at ~50 mN/m, even with the 21st cycle. Thus, Au NP markedly impeded both adsorption and the ability to attain γ_{min} near zero during either quasistatic or dynamic cycling.

Interaction of surfactant constituents with Au NP

The remarkable and unanticipated efficacy of NP to inhibit surfactant biophysical activity prompted further investigation on the interactions between Au NP and surfactant components. Initial studies examined the effects of individual surfactant PL molecular species on UV-vis absorption spectra. The effect of including the dimeric hydrophobic protein

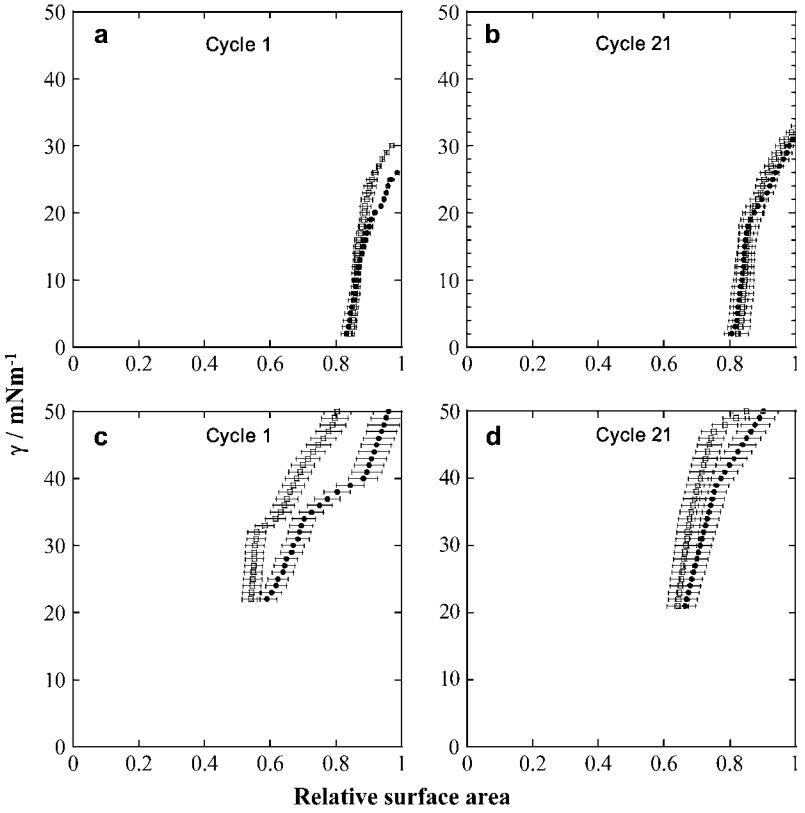

FIGURE 3 Dynamic compression (●)-expansion (○) isotherms of DPPC/POPG/SP-B during the first (*a* and *c*) and 21st (*b* and *d*) cycles in the absence (*a* and *b*) or presence (*c* and *d*) of blank Au NP (3.7 mol % PL).

SP-B, previously demonstrated to be essential for normal gaseous exchange (and therefore, life), with these lipids was also investigated.

As metal particle sizes decrease to the nanosize range there is a marked increase in surface plasmon resonance, which originates from the resonance of collective conduction electrons with incident electromagnetic radiation (32–35), resulting in a sharp elevation in absorbance in the visible region around 520 nm. The shape of the resonance peak is qualitatively related to the nature of the NP. Small, uniform NP with a narrow size distribution give a sharp absorbance, whereas a wide size distribution or any kind of aggregation leads to a broader absorbance. Fig. 4 depicts the UV-Vis absorbance of Au NP prepared with individual PLs (DPPC, POPG, DMPG, DPPG) in the presence or absence of SP-B. In each case, the POPG-, DMPG-, and DPPG-capped Au NP show a sharp plasmon resonance close to 530 nm, whereas DPPC-capped particles show a much broader absorbance that extends to longer wavelengths. Inclusion of 1% SP-B results in an instantaneous change in the ruby red color of the lipid-capped Au NP suspensions to purple, consistent with a decrease in the intensity at 520 nm with the appearance of a much broader peak, usually between 600 and 650 nm. This broader red-shifted adsorbance could arise from the emission of collective plasmon resonance caused by the aggregation of Au NP in the presence of SP-B.

The results in Fig. 4 are supported by TEM micrographs of lipid-capped Au NP formed in the presence or absence of SP-B. Fig. 5 shows that naked (*a* and *b*) and POPG-capped (*c* and *d*) Au NP have similar shape and size distributions, demonstrating that this PL does not interfere with NP growth. Both naked and POPG-capped NP appear predominantly present as single entities that are slightly aggregated. Most are rounded with diameters of 14.6 ± 3.8 ($n = 3$) and 17.4 ± 6.8 nm ($n = 3$) (Fig. 5, *b* and *d*). Closer inspection of

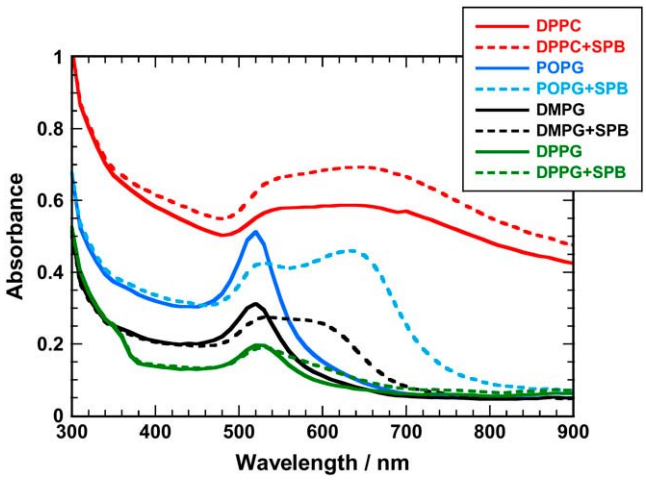

FIGURE 4 UV-visible spectra of aqueous lipid- (*top* to *bottom*, DPPC, POPG-, DMPG-, and DPPG-) capped gold nanoparticles in the presence and absence of surfactant protein B (1% wt/wt; see details in the text).

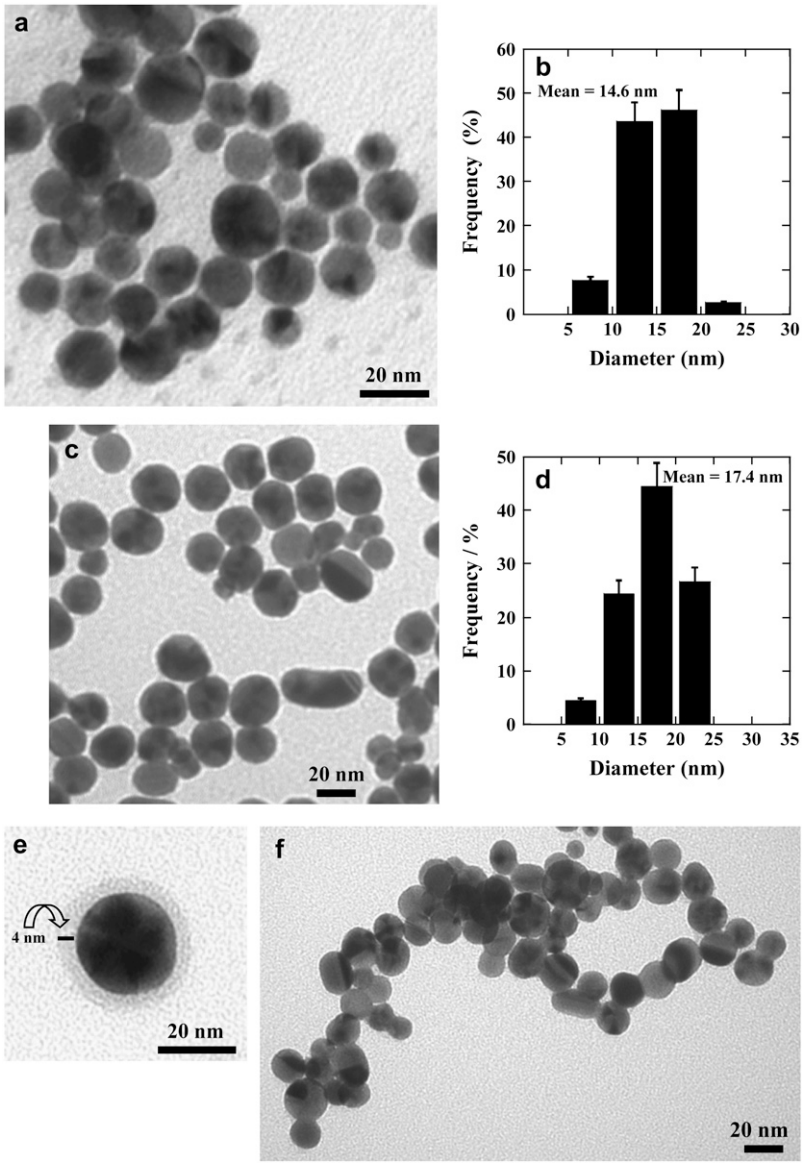

FIGURE 5 TEM micrographs of (*a*) blank (noncapped) Au NP and (*b*) POPG-capped Au NP prepared by the S-G procedure. The Au NP size distributions for (*c*) blank Au NP and (*d*) POPG-capped Au NP are depicted. An image consistent with the presence of a POPG bilayer around a single nanoparticle is shown in panel *e*. Strand formation induced by including 1% wt/wt SP-B with the POPG is shown in panel *f*.

the TEM images reveals that with POPG, Au NP can be enclosed with a thin coat of ~4 nm thickness (Fig. 5 *e*). A number of lipid membrane studies (36–40) have reported the thickness of PL bilayers to be ~4nm. Therefore, this observation is consistent with NP being covered with at least a single bilayer.

Fig. 5 *f* demonstrates the effect of adding SP-B where POPG-capped Au NP appeared to aggregate to form long threads or strands in the presence of this hydrophobic peptide. The strands seemed to be made of physically connected NP structures. In contrast to the loosely connected strings observed in the absence of SP-B, the strands are several particles thick in a number of places. In addition, with this sample, in some cases the particles appear to be in direct contact compared to Fig. 5 *b*, although this could reflect the tendency to pile up in layers. Somewhat similar TEM images were observed with DMPG, alone (Fig. 6 *a*) and in the presence of SP-B (Fig. 6 *b*). With DPPG, however, the particles appeared somewhat less regular in size and shape (Fig. 7 *a*) and addition of SP-B led to a tendency to aggregate rather than to form the elongated strands.

When DPPC was used as the capping agent, the shape of the NP became predominantly aspherical (Fig. 8). POPG, DMPG, and DPPG are the sodium salts of anionic PLs, whereas DPPC molecules are zwitterionic in nature. Ionic surfactant molecules are considered to be better capping agents than nonionic molecules since the former can provide both charge and steric stabilization (41–43) more effectively than the colloidal NP. Apart from this, although addition of SP-B showed some aggregation among the DPPC-capped NP (Fig. 8 *b*), no strands were found. The broad surface plasmon resonance observed for DPPC-capped NP in the

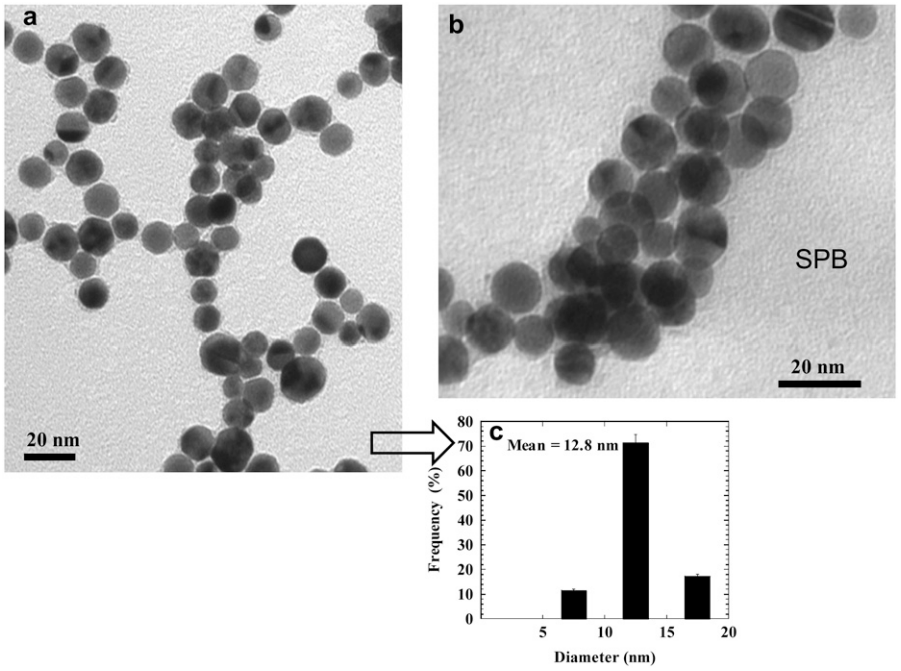

FIGURE 6 TEM micrographs of DMPG-capped Au NP in the absence (*a*) and presence (*b*) of SP-B (1% wt/wt DMPG). The size distributions of the NP in the absence of SP-B are depicted in panel *c*.

absence or in the presence of SP-B (Fig. 8) is consistent with the TEM observations.

The polarity of the lipid-capped NP can be examined with the help of gel electrophoresis (Fig. 9). Both POPG- and DMPG-capped NP move toward the positively charged electrode. Neither DPPC-capped nor DPPG-capped particles moved (data not shown). Interestingly, the addition of SP-B completely blocked movement of POPG- and DMPG-capped NP (Fig. 9). These results are consistent with the binding of the positively charged SP-B to the negatively charged lipid-capped NP resulting in large, relatively stable aggregates.

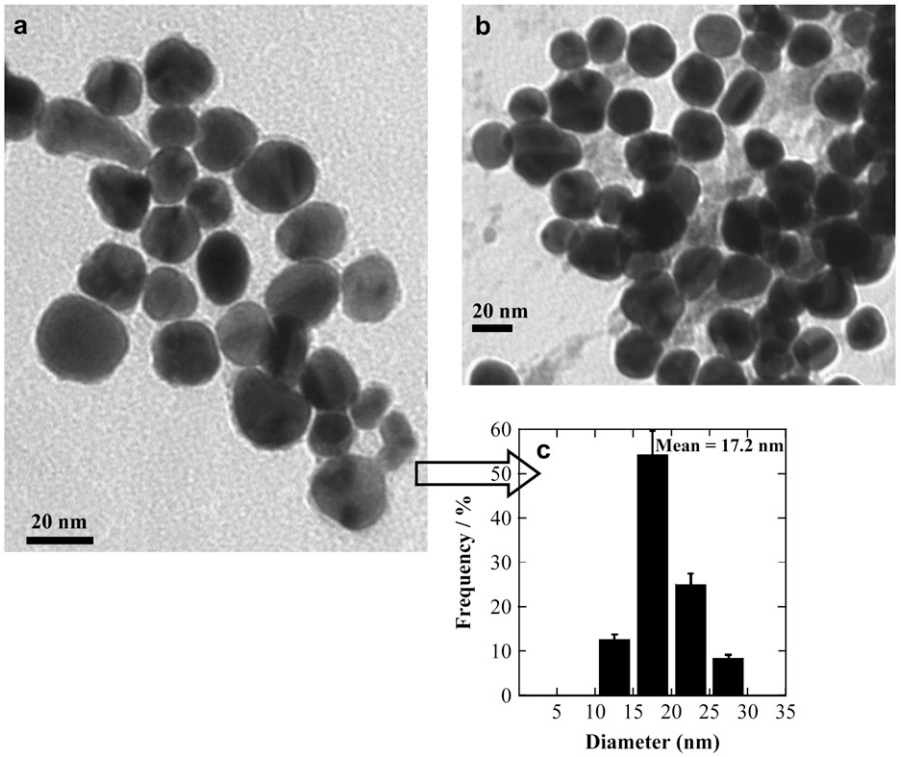

FIGURE 7 TEM micrographs of DPPG-capped Au NP in the absence (*a*) and presence (*b*) of 1% wt/wt SP-B. Size distribution of panel *a* is depicted in panel *c*.

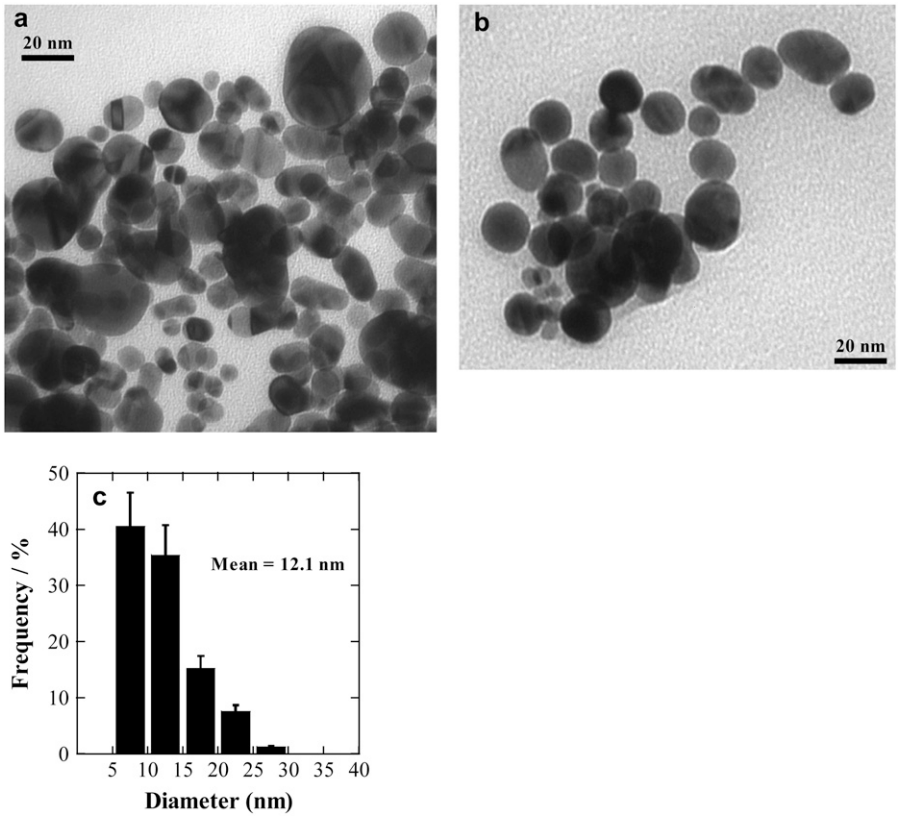

FIGURE 8 TEM micrographs of DPPC-capped Au NP in the absence (*a*) and presence (*b*) of 1% wt/wt PL SP-B. Note the presence of small and nonspherical NP. Size distribution of panel *a* is depicted in panel *c*.

DISCUSSION

Ultrafine air pollutants and pulmonary function

Epidemiological studies have reported that particulates associated with air pollutants contribute significantly to pulmonary and cardiovascular disease, resulting in higher levels of morbidity and mortality (14–18). Ultrafine particulates (i.e., $<$100 nm diameter) appear to be most potent (14,44,45). Studies to date have focused largely on asthma and emphysema. Previously reported investigations on surfactant normally involved relatively large particles. It should be noted that the results are highly variable and depend not only on the substance (i.e., cigarette smoke, diesel oil ash, wood ash, silica), but also on the nature of the study, even with the same material (44,46–49). It is apparent from these studies that secondary effects arising from interactions with lung cells are often involved in surfactant modifications and that reactive oxygen species can contribute.

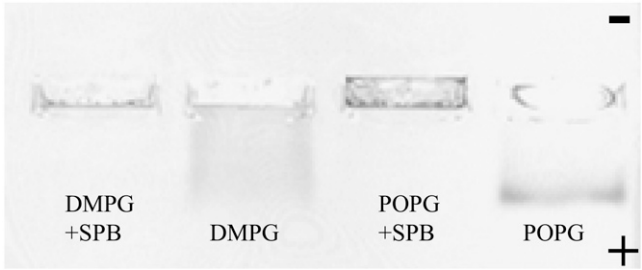

FIGURE 9 Gel electrophoresis showing the displacement of POPG- and DMPG-capped Au NP toward the positively charged electrode. Note the absence of any displacement of lipid-capped nanoparticles in the presence of 1% SP-B. No staining agent has been used.

Effect of Au NP on surfactant function

The potential effects of Au NP as air pollutants on pulmonary surfactant function was examined by mixing naked Au NP prepared by the S-G method, as indicated in the Experimental section, with DPPC/POPG/SP-B (70:30:1) and assaying PL adsorption and surfactant film surface activity during quasistatic and dynamic compression/expansion cycling with a CBT. Adding SP-B to DPPC/POPG resulted in a marked increase in PL absorption rate to the γ_{eq} of $\sim$23 mN/m. Further addition of Au NP at 3–7 mol % of PL, the lowest level examined markedly impeded surfactant adsorption. Adsorption was much slower than with PL in the absence of SP-B.

Surfactant PL adsorption is critical when an infant is born and for maintaining surfactant film levels to increase lung compliance and reduce the work of breathing. However, to maintain normal pulmonary function, surfactant films must achieve γ-values near zero during expiration (i.e., compression) and maintain γ-values near equilibrium during inspiration (i.e., surface area expansion) (1,3). In addition to

adsorption, addition of Au NP as low as 3.7 mol %, which corresponds to 0.98% w/w PL, also inhibited the ability of surfactant films to attain low γ-values during either quasistatic or dynamic compression.

Taken together, the results of these CBT studies demonstrate that inclusion of small amounts of Au NP dramatically alters the surface properties of the surfactant system in three distinct ways. First, Au NP interfere with the adsorption of PL to form a surface film at the γ_{eq} of ~23 mN/m (Fig. 1). Second, adding naked NP greatly hampers the ability of the surfactant system to lower γ during film compression so that γ_{min} increased to a value similar to the γ_{eq} of ~23 mN/m for this system during either quasistatic or dynamic cycling (Figs. 2 and 3). Such γ_{min} values could hamper optimal gaseous exchange in vivo (3). Third, the presence of NP interferes with the respreading of surfactant PL from surface collapse phases during film expansion in either quasistatic or dynamic cycling modes. Depressed PL respreading leads to a progressive increase in γ during compression/expansion cycling, at least potentially, leading to enhanced pulmonary edema (1,30). Thus, the presence of nanoparticles not only impedes the ability of pulmonary surfactant to adsorb to equilibrium, a process particularly critical at birth, but also obstructs the ability of the adsorbed surface films to attain low γ-values during compression and to maintain relatively low γ-values during expansion, properties that are crucial for preventing alveolar collapse.

Interactions between NP and surfactant constituents

Mammalian pulmonary surfactants contain ~80% PL (wt/wt), 5–10% neutral lipid (mainly cholesterol), and ~10% surfactant proteins. Surfactant PL are composed of ~80% PCs, ~12% PG, with smaller amounts of phosphatidylinositol, phosphatidylethanolamine, lyso-*bis*-phosphatidic acid, and sphingomyelin (50). The PC fraction contains 30–50% DPPC and the PG fraction contains ~10% DPPG. The TEM studies revealed diameters of Au NP grown in the presence of POPG (17.4 ± 3.0 nm, $n = 3$), DMPG (14.6 ± 7.2 nm, $n = 3$), or DPPG (17.2 ± 5.9 nm, $n = 3$) were similar to naked Au NP generated in the absence of lipid. The following scheme presents a plausible mechanism to explain Au NP capping. Growing Au NP from the seed solution are stabilized by negatively charged citrate ions. Under the conditions used, these could be released slowly, possibly accompanied by salt formation with sodium ions arising from the PG salts, as the citrate ions are replaced with negative charges from phosphate moieties in the acidic PG headgroups (51). Due to their amphipathic nature, PGs assembling on the particle would gain accompanying PGs, tail to tail, as directed by H_2O-repulsing energies arising from the hydrophobic effect. Consequently, Au NP would become covered with PGs, which in the case of POPG appear to form at least a single bilayer (Fig. 5 *e*). This conclusion is supported by cryotransmission electron microscopic studies by Mornet et al. (52), which demonstrated that silica NP are readily coated with a bilayer of neutral zwitterionic PCs and slightly negative PC/phosphatidylserine mixtures. Bilayer-protected Au NP have also been generated using the cationic detergent didodecyl dimethylammonium bromide (53) under conditions similar to those used here. The similar size distribution and uniform shapes of the Au NP grown in the presence and absence of fluid PGs indicate these PL layers are sufficiently permeable to allow particle growth to be completed during PG capping.

This appearance contrasts with that of Au NP grown in the presence of DPPC. Here, the size distribution was greatly altered, with large numbers of small, spherical NPs mixed with very large aspherical NPs (Fig. 8). The marked difference observed between PC and PG is consistent with previous studies, indicating ionic surfactant molecules are superior in contributing to both charge and steric stabilization (41–43,54). It appears that the zwitterionic DPPC inhibits accretion of Au molecules on some crystal planes, while leaving other crystal planes at least partially exposed for further growth in an anisotropic manner that generates many nonspherical NP.

It should be noted that in addition to affecting particle size and shape, zwitterionic DPPC-capped Au NP exhibited a different overall organization where the PC-capped particles appeared clumped in several layers. In addition, possibly because the layering made it more difficult to examine, Au NP capped with this saturated PC were not clearly separated.

These TEM images were obtained by evaporating aqueous droplets of Au NP on carbon-coated grids. Thus, it was not surprising that the NP tended to form single-layered clumps (Figs. 5, *a* and *b*, 6 *a*, and 7 *a*), which in some cases appeared as pearls on a string (e.g., Fig. 6 *a*). During these TEM studies, it was noticed that the overall distribution of PL-capped Au NP was influenced by including 1% SP-B (wt/wt). In all cases, in the presence of SP-B the fluid PG-capped NP formed elongated strand-like structures that were several layers thick in places. However, this transformation was considerably less evident with the DPPG-capped particles. Also, with DPPC-capped NP, particle strand formation could not be observed. Because the TEM samples are prepared by drying aqueous dispersions of the samples, the clumping and string formation observed could arise in part during drying. However, we were struck by the consistent appearance of thick Au NP strands, often several particles deep, with all of the samples containing SP-B and fluid PGs, but not in the other samples. These strands formed whether the Au NP were generated in the presence of PG/SP-B or the lipid/protein complex was added afterwards. These morphological changes are consistent with the well-recognized ability of SP-B to act as a ''fusogen'', as demonstrated by its ability to effectively destabilize bilayer integrity and morphology and promote lipid mixing (i.e., stimulate the interactions between lipid moieties present on the outer leaflet of bilayer vesicles) (5,55,56). These properties contribute to SP-B's role in the adsorption of sur-

factant from surface active films and the ability of such films to attain very low γ-values during compression.

Gel electrophoresis in agarose was also used to investigate the effect of SP-B on PL-capped Au NP. As anticipated, POPG- and DMPG-capped Au NP migrated toward the anode, although the latter NP exhibited considerable streaking. This may be attributed to the considerably higher gel/liquid crystalline bilayer T_c of the disaturated DMPG (25°C) relative to the unsaturated POPG (1°C) (57,58) and suggests fluidity is critical toward allowing the capped PG/Au complexes to migrate under the electromotive gradient. This presumably also explains the failure to observe complete capping of these NP with DPPG and DPPC bilayers. The observation that including 1% SP-B completely abolished migration of both POPG- and DMPG-capped Au NP indicates that the elongated strands shown in Figs. 5 and 6 are stable aggregates. This is consistent with the red shift observed with UV/vis. It should be noted that the immobility of SP-B-containing complexes cannot be attributed to the positive charges on SP-B. Mature SP-B contains eight positively and one negatively charged amino acid, but calculations show that under our conditions there are over 1000 negatively charged PG molecules per SP-B monomer. The aggregation to form long strands could result in the sequestering of surfactant lipids and SP-B in the hypophase.

The mechanisms involved in surfactant inhibition are not well understood. Surfactant inhibition by serum albumin, for example, is thought to occur through the ability of albumin to monopolize the surface (1,59). It is thought that the small size of albumin molecules enables them to adsorb rapidly and thereby hinder subsequent adsorption of surfactant PL. Separate studies conducted with a Wilhelmy plate demonstrated that Au NP are not surface active (data not shown). Thus, to interfere with surfactant function, Au NP would have to adsorb as coated particles. Studies conducted by others have demonstrated that laurylamine-coated and carboxylic acid terminated alkylthiol-derivatized Au NP can form monolayers (60,61). Furthermore, such monolayers are relatively unstable and did not reduce γ to below 50 mN/m during compression. However, there is no reason to anticipate more rapid adsorption of PL/SP-B-coated Au NP than of PL/SP-B vesicles alone. In addition, albumin inhibition requires higher concentrations of this protein than of the surfactant (59,62,63), but in this case there is a >25-fold excess of PL molecules over Au atoms. The PL molecules will be present in large aggregates, but the Au atoms are assembled into particles. Calculations show that Au NP of 15-Å diameter contain ~100,000 Au atoms, whereas Au NP of 20-Å diameter contain over 200,000 Au atoms. Thus, stochiometric considerations are complicated. In the absence of any theoretical reason or experimental evidence for selective adsorption of PL-coated Au NP and the relatively low concentration of these particles, we believe it unlikely that Au NP could inhibit pulmonary surfactant by monopolizing the air-liquid interface. Furthermore, unless γ rises above the equilibrium spreading γ of ~50 mN/m (60), albumin tends to be squeezed out of surfactant films and thus the inhibition overcome during film compression/expansion cycling. Thus, although lipid-capped Au NP can form monolayers, this inhibition mode is not consistent with the observed physicochemical surface characteristics.

Another inhibitory mechanism occurs with proteins, such as fibrinogen and C-reactive protein (CRP), which appear to inhibit surfactant by binding PL molecules (61–63). The inability of surfactant samples containing Au NP to reduce surface tension to below 20 mN/m during compression resembles the surface characteristics noted with CRP reasonably closely. Fibrinogen likely inhibits surfactant by precipitating surfactant PL and proteins. CRP is a pentamer of identical 24 kDa subunits, each of which can bind a single PC. Although the PC binding is presumably related to the inhibition of the adsorption of pulmonary surfactant films to attain low γ during compression, the manner is still not understood. This latter inhibition was observed with 50% CRP (wt/wt), whereas NP inhibition required <1% Au NP wt/wt of surfactant. The special properties of NP arise through the extremely large increase in a particle's surface area, which occurs as its diameter decreases. Consequently, our original interpretation of the results was that PL and possibly SP-B were sequestered on the Au NP surfaces and therefore less available for surface film formation. This could be considered analogous to the binding of PC by CRP. However, calculations based on the unit volume of Au atoms, the 3.7 mol % Au/PL, and assuming 70 $Å^2$ per PL molecule showed that the model pulmonary surfactant samples contain sufficient PL to cover particles of 15 nm with bilayers >1300-fold and particles of 20 nm diameter with bilayers >1700-fold.

The presence of this ''excess'' PL relative to Au NP made it apparent that Au NP possess a highly unusual ability to inhibit pulmonary surfactant and led us to seek an alternative explanation. The observation that addition of SP-B led to the formation of elongated strands with fluid PGs (Figs. 5 *f* and 6 *b*) provides a potential mechanism for sequestering surfactant SP-B and PG. This conclusion is supported by gel electrophoresis (Fig. 9), which shows SP-B induces strong aggregation of Au NP. In the absence of evidence for any other mechanism, we consider that the formation of such strands is the most probable basis for surfactant inhibition by low levels of Au NP.

Considerable evidence has accrued demonstrating that airborne pollutants can access and are retained by the terminal alveolar air spaces (64,65). Should Au NP become airborne either in the general environment or in the workplace, one can envision the following circumstance. Pulmonary surfactant adsorption to form a surface film normally occurs through unique vesicular structures known as tubular myelin. Au NP inhaled into the alveolar space during the breathing process could impact with such surface films, become wetted, and lined with PL bilayers (Fig. 10). These bilayers could remove PL from the surface monolayer and may or may not become enriched with PG due to specific interactions. Once in the subphase, coated particles would

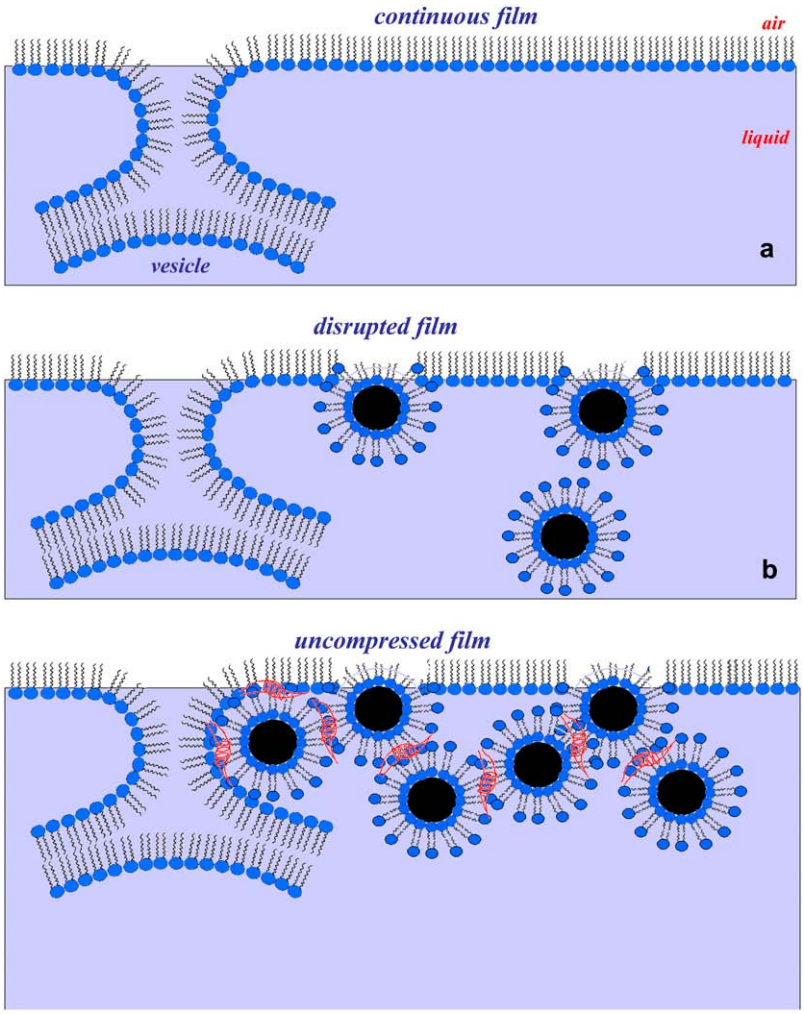

FIGURE 10 Potential scheme to explain potential inhibitory effects of Au NP on pulmonary surfactant in the alveolar space (not to scale). (*a*) A continuous surfactant film (monolayer and underlying multilayer) formed by the rupture of pulmonary surfactant vesicles at the air-liquid interface as the hypothetical rate-limiting intermediate structure between bilayer vesicles and the interfacial monolayer (see the literature (3,7,67) for further details). (*b*) The disrupted interfacial surfactant film due to the entrapping of Au NP (from the air phase as pollutants) by pulmonary surfactant. (*c*) The self-aggregation of lipid-capped Au NP in the presence of SP-B shown in red (see details in the text).

likely interact with SP-B either from the surface film or from lamellar bodies and could form structures similar to those observed by TEM. Elongated surfactant strands have been observed with surfactant films treated with residual oil fly ash particles arising from burning diesel oil (44), but whether these structures relate to the strands reported here and detected by TEM is not known. Surface balance studies have demonstrated that dusting DPPC monolayers with tantalum powder reduced their ability to lower γ to low values (66). The studies described here would suggest that elongated SP-B, PG, and Au NP-containing strands would not only sequester PL, impeding PL adsorption, but also inhibit the ability to attain the low γ-values required to stabilize alveoli during expiration. In addition, because respreading is poor, high γ-values $>$50 mN/m could arise, as observed in Figs. 2 and 3. This would subject the surface film to other inhibitors, such as serum proteins including albumin, which has been shown to interfere with surfactant function at high γ-values (60). At present, the fate of Au NP localized to the alveolar space is not known. The ultrafine particles derived from burnt diesel fuel have pulmonary half-lives in days (45). Au NP particles in the lung could be removed by lung macrophages, could be taken into the pulmonary interstitial cells, or could be absorbed into the blood stream (64,65). However, the likelihood exists that these particles could persist in the alveolar space for long periods.

None of the previously reported effects on pulmonary surfactant function appear to approach the dramatic effects on biophysical activity noted here. These studies would suggest that, through their ability to hamper surfactant function, ultrafine particles could also contribute to the development of ALI and ARDS. It must be emphasized that this does not mean that ultrafine particles necessarily act as the direct inducers of the pulmonary disease. Recent investigations have made it apparent that ALI or ARDS can arise as a result of a ''two-hit'' process, where the initial events predispose the lung to clinical expression of ALI (12,13). Hence, individuals subject to direct primary insult, such as acid aspiration, toxic gas inhalation, near-drowning, and hyperoxia, or indirect insults, such as systemic sepsis, massive trauma, multiple blood transfusions, alcoholism, and pancreatitis, may present with mild or negligible clinically relevant pulmonary inflamma-

tion. Nevertheless, when subject to a secondary event, which can be a second of the primary events listed above, or to other insults, such as mechanical ventilation, can result in a frank overwhelming (as opposed to a mild protective) primary response leading to ALI and ARDS. As stated earlier, the surfactant dysfunction usually accompanying these latter syndromes can act as a progressive factor. Given these and previous results indicating particulates and in particular ultrafine particles can impact negatively on surfactant function, it appears highly possible that ultrafine particles such as Au NP could act as a contributing factor to ALI and ARDS.

Concluding remarks

The continuing increases in air pollution have generated serious concern for human health. The respiratory system is the primary target of air pollutants, to which all human beings are exposed. This study examined the potential effects of metal NP, as a model air pollutant, on the surface activity of a semisynthetic pulmonary surfactant, DPPC/POPG/SP-B (70:30:1). The presence of Au NP at 3.7 mol %, 0.98 wt% (Au/PL) dramatically reduced the surface activity of this system. Both surfactant adsorption to form a surface film and the ability of this film to attain low γ-values during compression were compromised. A simple model has been presented to describe the potential behavior of NP at the air-liquid interface of the alveoli. These investigations were extended to examine interactions between Au NP and individual surfactant components. The results show that surfactant anionic PL have a strong affinity for Au NP and can cap Au NP in the form of one or likely more lipid bilayers, which provides charge and steric stabilization to colloidal NP. The presence of SP-B, which also interacts strongly with PG, leads to self-assembly of Au NP into elongated strand-like structures. This may be related to the fusogenic properties of this hydrophobic surfactant apoprotein. Similar observations resulted whether the Au NP were synthesized in the presence of PL or naked Au NP were added to an aqueous suspension of pulmonary surfactant. We expect a similar type of association between metal NP and pulmonary surfactants could occur when blank metal NP are inhaled during the normal breathing process. These results have possible relevance to the potential ability of ultrafine particulates to promote the development of ALI and ARDS.

The authors thank BLES Biochemicals, London, Ontario, Canada for BLES used for isolating the SP-B.

These studies were supported by grants MOP 66406 (F.P.) and FRN 15462 (N.O.P.) from the Canadian Institutes of Health Research.

REFERENCES

1. Possmayer, F. 2004. Physicochemical aspects of pulmonary surfactant. *In* Fetal and Neonatal Physiology. R. A. Polin, W. W. Fox, and S. H. Abman, editors. W. B. Saunders, Philadelphia, PA. 1014–1034.
2. Piknova, B., V. Schram, and S. Hall. 2002. Pulmonary surfactant: phase behavior and function. *Curr. Opin. Struct. Biol.* 12:487–494.
3. Bachofen, H., and S. Schurch. 2001. Alveolar surface forces and lung architecture. *Comp. Biochem. Physiol. A Mol. Integr. Physiol.* 129: 183–193.
4. Weaver, T. E., and J. J. Conkright. 2001. Function of surfactant proteins B and C. *Annu. Rev. Physiol.* 63:555–578.
5. Hawgood, S., M. Derrick, and F. Poulain. 1998. Structure and properties of surfactant protein B. *Biochim. Biophys. Acta.* 1408:150–160.
6. Johansson, J. 1998. Structure and properties of surfactant protein C. *Biochim. Biophys. Acta.* 1408:161–172.
7. Perez-Gil, J., and K. M. W. Keough. 1998. Interfacial properties of surfactant proteins. *Biochim. Biophys. Acta.* 1408:203–217.
8. McCormack, F. X., and J. A. Whitsett. 2002. The pulmonary collectins, SP-A and SP-D, orchestrate innate immunity in the lung. *J. Clin. Invest.* 109:707–712.
9. Haagsman, H. P., and R. V. Diemel. 2001. Surfactant-associated proteins: functions and structural variation. *Comp. Biochem. Physiol. A Mol. Integr. Physiol.* 129:91–108.
10. McCabe, A. J., D. T. Wilcox, B. A. Holm, and P. L. Glick. 2000. Surfactant—a review for pediatric surgeons. *J. Pediatr. Surg.* 35:1687–1700.
11. Pfister, R. H., and R. F. Soll. 2005. New synthetic surfactants: the next generation? *Biol. Neonate.* 87:338–344.
12. Lewis, J. F., and R. Veldhuizen. 2003. The role of exogenous surfactant in the treatment of acute lung injury. *Annu. Rev. Physiol.* 65: 613–642.
13. Lewis, J. F., and A. Brackenbury. 2003. Role of exogenous surfactant in acute lung injury. *Crit. Care Med.* 31:S324–S328.
14. Li, N., M. Hao, R. F. Phalen, W. C. Hinds, and A. E. Nel. 2003. Particulate air pollutants and asthma. A paradigm for the role of oxidative stress in PM-induced adverse health effects. *Clin. Immunol.* 109:250–265.
15. Buckeridge, D. L., R. Glazier, B. J. Harvey, M. Escobar, C. Amrhein, and J. Frank. 2002. Effect of motor vehicle emissions on respiratory health in an urban area. *Environ. Health Perspect.* 110:293–300.
16. Pope III, C. A., R. T. Burnett, M. J. Thun, E. E. Calle, D. Krewski, K. Ito, and G. D. Thurston. 2002. Lung cancer, cardiopulmonary mortality, and long-term exposure to fine particulate air pollution. *JAMA.* 287:1132–1141.
17. Samet, J. M., F. Dominici, F. C. Curriero, I. Coursac, and S. L. Zeger. 2000. Fine particulate air pollution and mortality in 20 U.S. cities, 1987–1994. *N. Engl. J. Med.* 343:1742–1749.
18. Gehr, P., F. H. Y. Green, M. Geiser, V. Im Hof, M. M. Lee, and S. Schurch. 1996. Airway surfactant, a primary defense barrier: mechanical and immunological aspects. *J. Aerosol Med.* 9:163–181.
19. Oberdorster, G., R. M. Gelein, J. Ferin, and B. Weiss. 1995. Association of particulate air pollution and acute mortality: involvement of ultrafine particles? *Inhal. Toxicol.* 7:111–124.
20. Bangham, A. D. 1998. Artificial lung expanding compound (ALEC-TM). *In* Medical Applications of Liposomes. D. Lasic and D. Papahadjopoulos, editors. Elsevier, Amsterdam, The Netherlands. 455–472.
21. Holm, B. A., A. R. Venkitaraman, G. Enhorning, and R. H. Notter. 1990. Biophysical inhibition of synthetic lung surfactants. *Chem. Phys. Lipids.* 52:243–250.
22. Zasadzinski, J. A., J. Ding, H. E. Warriner, F. Bringezu, and A. J. Waring. 2001. The physics and physiology of lung surfactants. *Curr. Opin. Colloid Interface Sci.* 6:506–513.
23. Keough, K. M. W. 1984. Physical chemical properties of some mixtures of lipids and their potential for use in exogenous surfactant. *Progr. Respir. Res.* 18:257–262.
24. Nag, K., J. G. Munro, K. Inchley, S. Schurch, N. O. Petersen, and F. Possmayer. 1999. SP-B refining of pulmonary surfactant phospholipid films. *Am. J. Physiol.* 277:L1179–L1189.

25. Yu, S.-H., and F. Possmayer. 1992. Effect of pulmonary surfactant protein B (SP-B) and calcium on phospholipid adsorption and squeeze-out of phosphatidylglycerol from binary phospholipid monolayers containing dipalmitoylphosphatidylcholine. *Biochim. Biophys. Acta.* 1126:26–34.

26. Yu, S. H., and F. Possmayer. 1993. Adsorption, compression and stability of surface films from natural, lipid extract and reconstituted pulmonary surfactants. *Biochim. Biophys. Acta.* 1167:264–271.

27. Yu, S. H., and F. Possmayer. 1994. Effect of pulmonary surfactant protein A (SP-A) and calcium on the adsorption of cholesterol and film stability. *Biochim. Biophys. Acta.* 1211:350–358.

28. Qanbar, R., S. Cheng, F. Possmayer, and S. Schurch. 1996. Role of the palmitoylation of surfactant-associated protein C in surfactant film formation and stability. *Am. J. Physiol.* 271:L572–L580.

29. Rodriguez-Capote, K., K. Nag, S. Schurch, and F. Possmayer. 2001. Surfactant protein interactions with neutral and acidic phospholipid films. *Am. J. Physiol. Lung Cell. Mol. Physiol.* 281:L231–L242.

30. Rodriguez-Capote, K., F. X. McCormack, and F. Possmayer. 2003. Pulmonary surfactant protein-A (SP-A) restores the surface properties of surfactant after oxidation by a mechanism that requires the Cys6 interchain disulfide bond and the phospholipid binding domain. *J. Biol. Chem.* 278:20461–20474.

31. Schoel, W. M., S. Schurch, and J. Goerke. 1994. The captive bubble method for the evaluation of pulmonary surfactant: surface tension, area, and volume calculations. *Biochim. Biophys. Acta.* 1200:281–290.

32. Liz-Marzan, L. M. 2006. Tailoring surface plasmons through the morphology and assembly of metal nanoparticles. *Langmuir.* 22:32–41.

33. Schultz, D. A. 2003. Plasmon resonant particles for biological detection. *Curr. Opin. Biotechnol.* 14:13–22.

34. Sun, Y., and Y. Xia. 2003. Gold and silver nanoparticles: a class of chromophores with colors tunable in the range from 400 to 750 nm. *Analyst.* 128:686–691.

35. Schofield, C. L., A. H. Haines, R. A. Field, and D. A. Russell. 2006. Silver and gold glyconanoparticles for colorimetric bioassays. *Langmuir.* 22:6707–6711.

36. Diemel, R. V., M. M. Snel, L. M. Van Golde, G. Putz, H. P. Haagsman, and J. J. Batenburg. 2002. Effects of cholesterol on surface activity and surface topography of spread surfactant films. *Biochemistry.* 41:15007–15016.

37. Saccani, J., S. Castano, B. Desbat, and D. Blaudez. 2003. A phospholipid bilayer supported under a polymerized Langmuir film. *Biophys. J.* 85:3781–3787.

38. Mitra, K., I. Ubarretxena-Belandia, T. Taguchi, G. Warren, and D. M. Engelman. 2004. Modulation of the bilayer thickness of exocytic pathway membranes by membrane proteins rather than cholesterol. *Proc. Natl. Acad. Sci. USA.* 101:4083–4088.

39. Blaurock, A. E., and T. J. McIntosh. 1986. Structure of the crystalline bilayer in the subgel phase of dipalmitoylphosphatidylglycerol. *Biochemistry.* 25:299–305.

40. McIntosh, T. J. 1980. Differences in hydrocarbon chain tilt between hydrated phosphatidylethanolamine and phosphatidylcholine bilayers. A molecular packing model. *Biophys. J.* 29:237–245.

41. Roucoux, A., J. Schulz, and H. Patin. 2002. Reduced transition metal colloids: a novel family of reusable catalysts? *Chem. Rev.* 102:3757–3778.

42. Napper, H. D. 1983. Polymeric Stabilization of Colloidal Dispersions. Academic Press, London, UK.

43. Lin, Y., and R. G. Finke. 1994. Novel polyoxoanion- and Bu_4N^+-stabilized, isolable, and redissolvable, 20–30-Å $Ir_{300–900}$ nanoclusters: the kinetically controlled synthesis, characterization, and mechanism of formation of organic solvent-soluble, reproducible size, and reproducible catalytic activity metal nanoclusters. *J. Am. Chem. Soc.* 116:8335–8353.

44. Anseth, J. W., A. J. Goffin, G. G. Fuller, A. J. Ghio, P. N. Kao, and D. Upadhyay. 2005. Lung surfactant gelation induced by epithelial cells exposed to air pollution or oxidative stress. *Am. J. Respir. Cell Mol. Biol.* 33:161–168.

45. Sioutas, C., R. J. Delfino, and M. Singh. 2005. Exposure assessment for atmospheric ultrafine particles (UFPs) and implications in epidemiologic research. *Environ. Health Perspect.* 113:947–955.

46. Gerber, P. J., C. Lehmann, P. Gehr, and S. Schurch. 2006. Wetting and spreading of a surfactant film on solid particles: influence of sharp edges and surface irregularities. *Langmuir.* 22:5273–5281.

47. Sosnowski, T. R., and A. Podgorski. 1999. Assessment of the pulmonary toxicity of inhaled gases and particles with physicochemical methods. *Int. J. Occup. Saf. Ergon.* 5:431–447.

48. Griese, M., G. Winzinger, A. Schams, M. Josten, A. Ziesenis, and K. Maier. 1999. Health effects of sulfur-related environmental air pollution: the pulmonary surfactant system is not disturbed by exposure to acidic sulfate and neutral sulfite aerosols. *J. Aerosol Med.* 12:37–44.

49. Subramaniam, S., J. A. Whitsett, W. Hull, and C. G. Gairola. 1996. Alteration of pulmonary surfactant proteins in rats chronically exposed to cigarette smoke. *Toxicol. Appl. Pharmacol.* 140:274– 280.

50. Lang, C. J., A. D. Postle, S. Orgeig, F. Possmayer, W. Bernhard, A. K. Panda, K. D. Jurgens, W. K. Milsom, K. Nag, and C. B. Daniels. 2005. Dipalmitoylphosphatidylcholine is not the major surfactant phospholipid species in all mammals. *Am. J. Physiol. Regul. Integr. Comp. Physiol.* 289:R1426–R1439.

51. Bakshi, M. S., P. Sharma, T. S. Banipal, G. Kaur, K. Torigoe, N. O. Petersen, and F. Possmayer. 2007. Lamellar phase supported synthesis of colloidal gold nanoparticles, nanoclusters, and nanowires formation. *J. Nanosci. Nanotechnol.* 7:916–924.

52. Mornet, S., O. Lambert, E. Duguet, and A. Brisson. 2005. The formation of supported lipid bilayers on silica nanoparticles revealed by cryoelectron microscopy. *Nano Lett.* 5:281–285.

53. Zhang, L., X. Sun, Y. Song, X. Jiang, S. Dong, and E. Wang. 2006. Didodecyldimethylammonium bromide lipid bilayer-protected gold nanoparticles: synthesis, characterization, and self-assembly. *Langmuir.* 22:2838–2843.

54. Bakshi, M. S., G. Kaur, P. Thakur, T. S. Banipal, F. Possmayer, and N. O. Petersen. 2007. Surfactant selective synthesis of gold nanowires by using a DPPC-surfactant mixture as a capping agent at ambient conditions. *J. Phys. Chem. C.* 111:5932–5940.

55. Hawgood, S. 2004. Surfactant protein B: structure and function. *Biol. Neonate.* 85:285–289.

56. Ryan, M. A., X. Qi, A. G. Serrano, M. Ikegami, J. Perez-Gil, J. Johansson, and T. E. Weaver. 2005. Mapping and analysis of the lytic and fusogenic domains of surfactant protein B. *Biochemistry.* 44:861–872.

57. Nagamachi, E., R. Kariyama, and Y. Kanemasa. 1985. The effect of head group structure on phase transition of phospholipid membranes as determined by differential scanning calorimetry. *Physiol. Chem. Phys. Med. NMR.* 17:255–260.

58. Wiedmann, T., A. Salmon, and V. Wong. 1993. Phase behavior of mixtures of DPPC and POPG. *Biochim. Biophys. Acta.* 1167:114–120.

59. Holm, B. A., Z. Wang, and R. H. Notter. 1999. Multiple mechanisms of lung surfactant inhibition. *Pediatr. Res.* 46:85–93.

60. Warriner, H. E., J. Ding, A. J. Waring, and J. A. Zasadzinski. 2002. A concentration-dependent mechanism by which serum albumin inactivates replacement lung surfactants. *Biophys. J.* 82:835–842.

61. Seeger, W., C. Grube, A. Gunther, and R. Schmidt. 1993. Surfactant inhibition by plasma proteins: differential sensitivity of various surfactant preparations. *Eur. Respir. J.* 6:971–977.

62. McEachren, T. M., and K. M. Keough. 1995. Phosphocholine reverses inhibition of pulmonary surfactant adsorption caused by C-reactive protein. *Am. J. Physiol.* 269:L492–L497.

63. Nag, K., K. Rodriguez-Capote, A. K. Panda, L. Frederick, S. A. Hearn, N. O. Petersen, S. Schurch, and F. Possmayer. 2004. Disparate effects

of two phosphatidylcholine binding proteins, C-reactive protein and surfactant protein A, on pulmonary surfactant structure and function. *Am. J. Physiol. Lung Cell. Mol. Physiol.* 287:L1145–L1153.

64. Gehr, P., F. Blank, and B. M. Rothen-Rutishauser. 2006. Fate of inhaled particles after interaction with the lung surface. *Paediatr. Respir. Rev.* 7(Suppl. 1):S73–S75.
65. Geiser, M., B. Rothen-Rutishauser, N. Kapp, S. Schurch, W. Kreyling, H. Schulz, M. Semmler, V. Im Hof, J. Heyder, and P. Gehr. 2005. Ultrafine particles cross cellular membranes by nonphagocytic mechanisms in lungs and in cultured cells. *Environ. Health Perspect.* 113:1555–1560.
66. Schurch, S. F., and M. R. Roach. 1976. Interference of bronchographic agents with lung surfactant. *Respir. Physiol.* 28:99–117.
67. Biswas, S. C., S. B. Rananavare, and S. B. Hall. 2007. Differential effects of lysophosphatidylcholine on the adsorption of phospholipids to an air/water interface. *Biophys. J.* 92:493–501.